Journal of Systems Engineering and Electronics
Vol. 33, No. 4, August 2022, pp.887 – 895

Joint angle and frequency estimation for linear array: an extended DOA-matrix method

CHEN Luo[1,2], DAI Xiangrui[1,*], and ZHANG Xiaofei[1]

1. College of Electronic and Information Engineering, Nanjing University of Aeronautics and Astronautics, Nanjing 210016, China;
2. The 28th Research Institute of China Electronics Technology Group Corporation, Nanjing 210007, China

Abstract: An approach for joint direction of arrival (DOA) angle and frequency estimation for a linear array is investigated in this paper. Specifically, we make the utmost of the autocorrelation and cross-correlation information to propose an extended DOA-matrix (EDOAM) method. Subsequently, we obtain the auto-paired angle and frequency estimates by the eigenvalues and the corresponding eigenvectors of the novel DOA matrix. Furthermore, the proposed method surpasses the DOA-matrix method which partly ignores the autocorrelation and cross-correlation information. Finally, the proposed method works well for both uniform and non-uniform linear arrays. The simulation consequences indicate the superiority of our proposed approach.

Keywords: direction of arrival (DOA), frequency, linear array, time delay, extended DOA-matrix method.

DOI: 10.23919/JSEE.2022.000086

1. Introduction

Array multi-parameter estimation is an essential problem in array signal processing. Joint estimation of frequency, Doppler shift, direction of arrival (DOA) and time/time difference of arrival (TDOA) is a standard application in multi-parameter estimation. Up to now, joint angle and frequency estimation is of great significance for various applications such as radar and wireless communication [1−5].

Over the decades, DOA estimation has become a hot topic. Many high accuracy algorithms have been presented, which include multi-dimensional multiple signal classification (MUSIC) algorithm [6], estimating signal parameters via rotational invariance techniques (ESPRIT) algorithm [7], Capon algorithm [8], Propagator method (PM) [9], maximum likelihood (ML) method [10], and DOA matrix (DOAM) method [11,12]. Among these methods, the MUSIC algorithm and the ML method can achieve better estimation accuracy, but their computational complexity is higher. While the ESPRIT algorithm and the PM have elevated computational efficiency, their estimation performance has been satisfactorily evaluated.

Since the introduction of the least-squares (LS) method of the frequency-wave number, many conventional algorithms, such as linear prediction method for azimuth-frequency joint estimation [1], MUSIC algorithm [13−15], ESPRIT algorithm [16,17], PM algorithm [18], ML method [19] and DOAM method [20], have been applied into the estimation of joint angle and frequency [13−31]. Moreover, Zoltowski et al. considered the problem of joint two-dimensional (2-D) DOA and frequency estimation in radar signal processing and application fields [2] while Haardt et al. discussed joint 2-D DOA and frequency estimation in the field of mobile communication [3]. In order to reduce the amount of algorithm calculation, Zoltowski et al. designed a novel algorithm based on the unitary-ESPRIT algorithm which converts the data matrix into a real matrix by Cayley transform [21].

In [11], Yin et al. proposed the DOAM approach for 2-D DOA angle estimation with two parallel linear arrays. Specifically, the DOAM method structures a matrix through the auto-correlation matrix and the cross-correlation matrix, and then the 2-D DOA angle estimates can then be calculated by executing eigenvalue decomposition (EVD) to the matrix. Since peak search is not required, the DOAM method has a lower computational complexity than the MUSIC algorithm. However, the DOAM method partly ignores the auto-correlation and cross-correlation information, which internally degenerates the estimation precision. To tackle this problem, Dai et al. proposed an extended DOAM (EDOAM) method, where an extended matrix that involves all the auto-

Manuscript received February 26, 2020.
*Corresponding author.
This work was supported by the National Natural Science Foundation of China (61971217;61971218;61631020), Jiangsu Natural Science Foundation (BK20200444), Jiangsu Key Research and Development Project (BE2020101), and the Fund of Sonar Technology Key Laboratory.

correlation and cross-correlation information is constructed [22].

In this paper, we combine the EDOAM method with linear arrays and derive an efficient joint DOA and frequency estimation method. Specifically, we perform EVD on the EDOAM. Then, the estimation of the frequency as well as the DOA can be obtained with the resulting eigenvalues and eigenvectors. We have evaluated the angle and frequency estimation performance by extensive Monte Carlo simulations. The simulation consequences show that the proposed EDOAM approach exhibits higher angle and frequency estimation precision than the DOAM method.

The main contributions of our research are summarized as follows:

(i) To solve the problem of joint estimation of angle and frequency, we propose an EDOAM method.

(ii) We adequately utilize auto-correlation and cross-correlation information to construct the EDOAM, while the DOAM method partly exploits the information.

(iii) The EDOAM method has a better angle and frequency estimation performance than the DOAM method.

2. Data model

Suppose there are K uncorrelated far-field narrowband sources impinging on an M-sensor linear array as shown in Fig. 1. We define the first array element as the origin array element and $d_k(k=0,1,\cdots,M-1)$ as the distance between the mth element and the origin element, where $d_0=0$. Each element is connected to a delay unit with delay of τ as shown in Fig. 2. Assume that $\theta_i(i=1,2,\cdots,K)$ is the elevation angle and $f_i(i=1,2,\cdots,K)$ is the carrier frequency of the ith source.

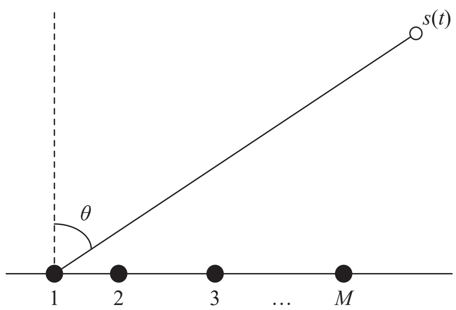

Fig. 1 Linear array

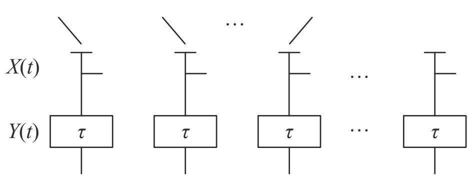

Fig. 2 Signal receiving system with single delay

Remark 1 In this paper, we assume that these sources are uncorrelated. If these sources are correlated, we can use spatial smoothing technology to complete decorrelation.

The received signal of the mth $(1,2,\cdots,M)$ array element and the corresponding time delay unit [15] are

$$x_m(t)=\sum_{i=1}^{K}\exp\left[-\mathrm{j}2\pi d_m f_i\frac{\sin\,\theta_i}{\mathrm{c}}\right]s_i(t)+n_i(t), \tag{1}$$

$$\begin{aligned} y_m(t)&=x_m(t-\tau)= \\ &\sum_{i=1}^{K}\exp\left[-\mathrm{j}2\pi d_m f_i\frac{\sin\,\theta_i}{\mathrm{c}}\right]s_i(t-\tau)+n_i(t-\tau), \end{aligned} \tag{2}$$

where c is the transmission speed of electromagnetic wave, and $n_i(t)$ is the array output noise. Hence, after vectori-zation [15], we can obtain

$$\boldsymbol{x}(t)=\boldsymbol{A}\mathbf{s}(t)+\boldsymbol{n}(t), \tag{3}$$

$$\begin{aligned} \boldsymbol{y}(t)&=\boldsymbol{A}\boldsymbol{s}(t-\tau)+\boldsymbol{n}(t-\tau)= \\ &\boldsymbol{A}\boldsymbol{\Gamma}\boldsymbol{s}(t)+\boldsymbol{n}(t-\tau), \end{aligned} \tag{4}$$

where $\boldsymbol{x}(t)=[x_1(t),x_2(t),\cdots,x_M(t)]^{\mathrm{T}}$, $\boldsymbol{y}(t)=[y_1(t),y_2(t),\cdots,y_M(t)]^{\mathrm{T}}$, $\boldsymbol{s}(t)=[s_1(t),s_2(t),\cdots,s_K(t)]^{\mathrm{T}}$. $\boldsymbol{n}(t)=[n_1(t),n_2(t),\cdots,n_M(t)]^{\mathrm{T}}$ represents the additive white Gaussian noise vector, where mean is zero and variance is σ^2. $\boldsymbol{\Gamma}$ denotes the steering matrix which can be given by

$$\boldsymbol{\Gamma}=\mathrm{diag}\{\exp(-\mathrm{j}2\pi f_1\tau),\cdots,\exp(-\mathrm{j}2\pi f_K\tau)\}. \tag{5}$$

The steering matrix of the array is $\boldsymbol{A}=[\boldsymbol{a}(f_1,\theta_1),\boldsymbol{a}(f_2,\theta_2),\cdots,\boldsymbol{a}(f_K,\theta_K)]$, where

$$\boldsymbol{a}(f_k,\theta_k)=\begin{bmatrix} 1 \\ \exp\left(-\mathrm{j}2\pi f_k d_1\dfrac{\sin\,\theta_k}{\mathrm{c}}\right) \\ \vdots \\ \exp\left(-\mathrm{j}2\pi f_k d_{M-1}\dfrac{\sin\,\theta_k}{\mathrm{c}}\right) \end{bmatrix},$$

$$k=1,2,\cdots,K. \tag{6}$$

3. Joint angle and frequency estimation via DOAM method

According to the received data of the signal receiving system, we can derive four auto-correlation and cross-correlation matrices of $\boldsymbol{x}(t)$ and $\boldsymbol{y}(t)$. However, the conventional DOAM method only uses the auto-correlation matrix of $\boldsymbol{x}(t)$ and the cross-correlation matrix of $\boldsymbol{y}(t)$ and $\boldsymbol{x}(t)$ [11] defined by

$$\boldsymbol{R}_{xx}=\mathrm{E}[\boldsymbol{x}(t)\boldsymbol{x}^{\mathrm{H}}(t)]=\boldsymbol{A}\boldsymbol{\Psi}\boldsymbol{A}^{\mathrm{H}}+\sigma^2\boldsymbol{I}, \tag{7}$$

$$\boldsymbol{R}_{yx} = \mathrm{E}[\boldsymbol{y}(t)\boldsymbol{x}^{\mathrm{H}}(t)] = \boldsymbol{A}\boldsymbol{\Gamma}\boldsymbol{\Psi}\boldsymbol{A}^{\mathrm{H}}, \tag{8}$$

where $\boldsymbol{\Psi} = \mathrm{E}[\boldsymbol{s}(t)\boldsymbol{s}^{\mathrm{H}}(t)]$ represents the covariance matrix of the signals.

To estimate the variance of noise, we perform EVD to $\boldsymbol{R}_{xx}$ and obtain the eigenvalues $\varepsilon_1, \varepsilon_2, \cdots, \varepsilon_M$, where $\varepsilon_1 > \cdots > \varepsilon_K > \cdots > \varepsilon_M$. Hence, the noise variance can be calculated as $\hat{\sigma}^2 = (\varepsilon_{K+1} + \cdots + \varepsilon_M)/(M-K)$. Therefore, we can eliminate the impact of noise [11] as

$$\boldsymbol{C}_{xx} = \boldsymbol{R}_{xx} - \hat{\sigma}^2\boldsymbol{I} = \boldsymbol{A}\boldsymbol{\Psi}\boldsymbol{A}^{\mathrm{H}}. \tag{9}$$

Define the DOA matrix $\boldsymbol{R} \in \boldsymbol{C}^{M\times M}$ [11] as

$$\boldsymbol{R} = \boldsymbol{R}_{yx}\boldsymbol{C}_{xx}^{+} \tag{10}$$

where $\boldsymbol{C}_{xx}^{+}$ represents the pseudo-inverse of $\boldsymbol{C}_{xx}$.

Theorem 1 If $\boldsymbol{A}$ and $\boldsymbol{\Psi}$ are nonsingular, then the signal frequency elements are equal to the K non-zero unequal eigenvalues of $\boldsymbol{R}$, and the corresponding eigenvectors are equal to the signal direction vectors [11], i.e.,

$$\boldsymbol{R}\boldsymbol{A} = \boldsymbol{A}\boldsymbol{\Gamma}. \tag{11}$$

Hence, frequency estimation can be achieved by the eigenvalues of $\boldsymbol{R}$, and angle estimation can be achieved by the corresponding eigenvectors. The correspondence relation realizes the auto-pair of angle and frequency.

4. Joint angle and frequency estimation via EDOAM

The conventional DOAM method underutilizes the auto-correlation and cross-correlation information of received data leading to the degradation of the DOA and frequency estimation performance. In this paper, we propose an extended estimation method based on the conventional DOAM method, which makes the utmost use of the information in the four auto-correlation and cross-correlation matrices. The auto-correlation matrix and cross-correlation matrix of $\boldsymbol{y}(t)$ and $\boldsymbol{x}(t)$ can be denoted [22] as

$$\begin{aligned}\boldsymbol{R}_{yy} &= \mathrm{E}[\boldsymbol{y}(t)\boldsymbol{y}^{\mathrm{H}}(t)] = \boldsymbol{A}\boldsymbol{\Gamma}\boldsymbol{\Psi}\boldsymbol{\Gamma}^{\mathrm{H}}\boldsymbol{A}^{\mathrm{H}} + \sigma^2\boldsymbol{I} = \\ &\boldsymbol{A}\boldsymbol{\Psi}\boldsymbol{\Gamma}\boldsymbol{\Gamma}^{\mathrm{H}}\boldsymbol{A}^{\mathrm{H}} + \sigma^2\boldsymbol{I} = \boldsymbol{A}\boldsymbol{\Psi}\boldsymbol{A}^{\mathrm{H}} + \sigma^2\boldsymbol{I},\end{aligned} \tag{12}$$

$$\boldsymbol{R}_{xy} = \mathrm{E}[\boldsymbol{x}(t)\boldsymbol{y}^{\mathrm{H}}(t)] = \boldsymbol{A}\boldsymbol{\Gamma}^{\mathrm{H}}\boldsymbol{\Psi}\boldsymbol{A} = \boldsymbol{A}\boldsymbol{\Gamma}^{-1}\boldsymbol{\Psi}\boldsymbol{A}. \tag{13}$$

According to the relation between the auto-correlation matrix and the cross-correlation matrix, we define two novel matrices $\boldsymbol{R}_1, \boldsymbol{R}_2 \in \mathbf{C}^{2M\times M}$ which contain all the auto-correlation and cross-correlation information, i.e.,

$$\boldsymbol{R}_1 = \begin{bmatrix} \boldsymbol{C}_{xx} \\ \boldsymbol{R}_{xy} \end{bmatrix} = \begin{bmatrix} \boldsymbol{A}\boldsymbol{\Psi}\boldsymbol{A}^{\mathrm{H}} \\ \boldsymbol{A}\boldsymbol{\Gamma}^{-1}\boldsymbol{\Psi}\boldsymbol{A}^{\mathrm{H}} \end{bmatrix}, \tag{14}$$

$$\boldsymbol{R}_2 = \begin{bmatrix} \boldsymbol{R}_{yx} \\ \boldsymbol{C}_{yy} \end{bmatrix} = \begin{bmatrix} \boldsymbol{A}\boldsymbol{\Gamma}\boldsymbol{\Psi}\boldsymbol{A}^{\mathrm{H}} \\ \boldsymbol{A}\boldsymbol{\Psi}\boldsymbol{A}^{\mathrm{H}} \end{bmatrix}, \tag{15}$$

where $\boldsymbol{C}_{yy} = \boldsymbol{A}\boldsymbol{\Psi}\boldsymbol{A}^{\mathrm{H}} = \boldsymbol{R}_{yy} - \sigma^2\boldsymbol{I}$.

We define a matrix $\boldsymbol{A}_E \in \mathbf{C}^{2M\times K}$ [22] as

$$\boldsymbol{A}_E = \begin{bmatrix} \boldsymbol{A} \\ \boldsymbol{A}\boldsymbol{\Gamma}^{-1} \end{bmatrix}. \tag{16}$$

Hence

$$\boldsymbol{R}_1 = \boldsymbol{A}_E\boldsymbol{\Psi}\boldsymbol{A}^{\mathrm{H}}, \tag{17}$$

$$\boldsymbol{R}_2 = \boldsymbol{A}_E\boldsymbol{\Gamma}\boldsymbol{\Psi}\boldsymbol{A}^{\mathrm{H}}. \tag{18}$$

Therefore, similar to the traditional DOA matrix, an extended DOA matrix can be defined [22] as

$$\boldsymbol{R}_E = \boldsymbol{R}_2\boldsymbol{R}_1^{+} = \begin{bmatrix} \boldsymbol{R}_{yx} \\ \boldsymbol{C}_{yy} \end{bmatrix}\begin{bmatrix} \boldsymbol{C}_{xx} \\ \boldsymbol{R}_{xy} \end{bmatrix}^{+} \tag{19}$$

where $\boldsymbol{R}_1^{+} = \boldsymbol{R}_1^{\mathrm{H}}(\boldsymbol{R}_1\boldsymbol{R}_1^{\mathrm{H}})^{-1}$ is the pseudo-inverse of $\boldsymbol{R}_1$. $\boldsymbol{R}_E$ contains all the auto-correlation and cross-correlation information. $[\cdot]^{+}$ represents the pseudoinverse of a matrix or rector.

Lemma 1 If $\boldsymbol{A}$ and $\boldsymbol{\Psi}$ are nonsingular, the signal frequency elements of $\boldsymbol{\Gamma}$ are equal to the K non-zero unequal eigenvalues of $\boldsymbol{R}_E$, and the corresponding eigenvectors are equal to the signal direction vectors, i.e.,

$$\boldsymbol{R}_E\boldsymbol{A}_E = \boldsymbol{A}_E\boldsymbol{\Gamma}. \tag{20}$$

Proof According to (17), we can obtain

$$\boldsymbol{\Psi}\boldsymbol{A}^{\mathrm{H}} = (\boldsymbol{A}_E^{\mathrm{H}}\boldsymbol{A}_E)^{-1}\boldsymbol{A}_E^{\mathrm{H}}\boldsymbol{R}_1, \tag{21}$$

Substitute (21) into (18),

$$\boldsymbol{R}_2 = \boldsymbol{A}_E\boldsymbol{\Gamma}(\boldsymbol{A}_E^{\mathrm{H}}\boldsymbol{A}_E)^{-1}\boldsymbol{A}_E^{\mathrm{H}}\boldsymbol{R}_1. \tag{22}$$

We define the matrix $\boldsymbol{T} = \boldsymbol{\Psi}\boldsymbol{A}^{\mathrm{H}}$. According to the properties and theorems of the rank of matrices, we can obtain $\mathrm{rank}(\boldsymbol{A}_E \in \mathbf{C}^{2M\times K}) = K$ and $\mathrm{rank}(\boldsymbol{T} \in \mathbf{C}^{K\times M}) = K$, we define $\boldsymbol{R}_1^{+}$ [25] as

$$\begin{aligned}\boldsymbol{R}_1^{+} &= \boldsymbol{T}^{\mathrm{H}}(\boldsymbol{T}\boldsymbol{T}^{\mathrm{H}})^{-1}(\boldsymbol{A}_E^{\mathrm{H}}\boldsymbol{A}_E)^{-1}\boldsymbol{A}_E^{\mathrm{H}} = \\ &\boldsymbol{A}\boldsymbol{\Psi}^{\mathrm{H}}(\boldsymbol{\Psi}\boldsymbol{A}^{\mathrm{H}}\boldsymbol{A}\boldsymbol{\Psi}^{\mathrm{H}})^{-1}(\boldsymbol{A}_E^{\mathrm{H}}\boldsymbol{A}_E)^{-1}\boldsymbol{A}_E^{\mathrm{H}}.\end{aligned} \tag{23}$$

Therefore,

$$\begin{aligned}\boldsymbol{R}_1\boldsymbol{R}_1^{+} &= \boldsymbol{A}_E\boldsymbol{\Psi}\boldsymbol{A}^{\mathrm{H}}\boldsymbol{A}\boldsymbol{\Psi}^{\mathrm{H}}(\boldsymbol{\Psi}\boldsymbol{A}^{\mathrm{H}}\boldsymbol{A}\boldsymbol{\Psi}^{\mathrm{H}})^{-1}(\boldsymbol{A}_E^{\mathrm{H}}\boldsymbol{A}_E)^{-1}\boldsymbol{A}_E^{\mathrm{H}} = \\ &\boldsymbol{A}_E(\boldsymbol{A}_E^{\mathrm{H}}\boldsymbol{A}_E)^{-1}\boldsymbol{A}_E^{\mathrm{H}}.\end{aligned} \tag{24}$$

Then according to (19), we can obtain

$$\begin{aligned}\boldsymbol{R}_2\boldsymbol{R}_1^{+}\boldsymbol{A}_E &= \boldsymbol{A}_E\boldsymbol{\Gamma}(\boldsymbol{A}_E^{\mathrm{H}}\boldsymbol{A}_E)^{-1}\boldsymbol{A}_E^{\mathrm{H}}\boldsymbol{R}_1\boldsymbol{R}_1^{+}\boldsymbol{A}_E = \\ &\boldsymbol{A}_E\boldsymbol{\Gamma}(\boldsymbol{A}_E^{\mathrm{H}}\boldsymbol{A}_E)^{-1}\boldsymbol{A}_E^{\mathrm{H}}\boldsymbol{A}_E = \boldsymbol{A}_E\boldsymbol{\Gamma}.\end{aligned} \tag{25}$$

Thus, we have $\boldsymbol{R}_E\boldsymbol{A}_E = \boldsymbol{A}_E\boldsymbol{\Gamma}$. □

Therefore, by implementing EVD on $\boldsymbol{R}_E$, we can obtain $\hat{\boldsymbol{A}}_E$ and $\hat{\boldsymbol{\Gamma}}$ which are the estimates of $\boldsymbol{A}_E$ and $\boldsymbol{\Gamma}$. Hence, the estimates of the frequency can be achieved from the eigenvalues $\lambda_1, \lambda_2, \cdots, \lambda_K$, then the corresponding direction vector estimations are realized by the corresponding feature vectors $\boldsymbol{v}_1, \boldsymbol{v}_2, \cdots, \boldsymbol{v}_K$, hence the correspondence automatically realizes direction and frequency pairing.

The frequency estimation can be obtained by

$$\hat{f}_k = -\text{angle}\left(\frac{\lambda_k}{2\pi\tau}\right). \tag{26}$$

On account of $\hat{\boldsymbol{A}}_E$ and (16), we divide $\hat{\boldsymbol{A}}_E$ into $\hat{\boldsymbol{A}}_1$ and $\hat{\boldsymbol{A}}_2$, where $\hat{\boldsymbol{A}}_1 \in \mathbf{C}^{M\times K}$ is composed of the first to the Mth row of $\hat{\boldsymbol{A}}_E$, and $\hat{\boldsymbol{A}}_2 \in \mathbf{C}^{M\times K}$ contains the $(M+1)$th to $(2M)$th row of $\hat{\boldsymbol{A}}_E$. $\hat{\boldsymbol{A}}_1$ and $\hat{\boldsymbol{A}}_2$ are the estimates of $\boldsymbol{A}$ and $\boldsymbol{A\Gamma}^{-1}$, respectively.

Then we compute the angle by $\hat{\boldsymbol{A}}_1$. The direction vector of the kth signal is

$$\boldsymbol{a}(\theta_k) = \left[1, \mathrm{e}^{-\mathrm{j}2\pi d_1 f_k \frac{\sin\theta_k}{\mathrm{c}}}, \cdots, \mathrm{e}^{-\mathrm{j}2\pi d_{M-1} f_k \frac{\sin\theta_k}{\mathrm{c}}}\right]^{\mathrm{T}}. \tag{27}$$

Hence

$$\boldsymbol{u}_k = -\text{angle}(\boldsymbol{a}(\theta_k)) = \left[0, 2\pi d_1 f_k \frac{\sin\theta_k}{\mathrm{c}}, \cdots, 2\pi d_{M-1} f_k \frac{\sin\theta_k}{\mathrm{c}}\right]^{\mathrm{T}}. \tag{28}$$

Normalize the kth eigenvector $\boldsymbol{v}_k$ to get $\boldsymbol{v}'_k$ and $\hat{\boldsymbol{u}}_k = -\text{angle}(\boldsymbol{v}'_k)$, then the LS can be fitted as

$$\boldsymbol{P}_k \boldsymbol{e}_k = \hat{\boldsymbol{u}}_k \tag{29}$$

where

$$\begin{cases} \boldsymbol{P}_k = \begin{bmatrix} 1 & 0 \\ 1 & 2\pi d_1 \dfrac{\hat{f}_k}{\mathrm{c}} \\ \vdots & \vdots \\ 1 & 2\pi d_{M-1} \dfrac{\hat{f}_k}{\mathrm{c}} \end{bmatrix} \\ \boldsymbol{e}_k = \begin{bmatrix} e_0 \\ e_1 \end{bmatrix} \end{cases} \tag{30}$$

where $\hat{f}_k$ is the estimation of the frequency and $e_1 = \sin\theta_k$.

The LS solution of $\boldsymbol{e}_k$ can be obtained by

$$\hat{\boldsymbol{e}}_k = (\boldsymbol{P}_1^{\mathrm{T}} \boldsymbol{P}_1)^{-1} \boldsymbol{P}_1^{\mathrm{T}} \hat{\boldsymbol{u}}_k. \tag{31}$$

Then the estimation of angles can be achieved by

$$\hat{\theta}_{k1} = \arcsin \hat{e}_1, \ k = 1, 2, \cdots, K. \tag{32}$$

Furthermore, we calculate another estimate of angle $\hat{\theta}_{k2}$ by $\hat{\boldsymbol{A}}_2 \hat{\boldsymbol{\Gamma}}$. Hence, the estimation of DOA can be achieved by

$$\hat{\theta}_k = \frac{\hat{\theta}_{k1} + \hat{\theta}_{k2}}{2}. \tag{33}$$

In summary, the major flow of the method proposed in this paper can be generalized as follows:

Step 1 Compute the auto-correlation and cross-correlation matrices:

$$\hat{\boldsymbol{R}}_{xx} = \frac{1}{N}\sum_{n=1}^{N} \boldsymbol{x}(t)\boldsymbol{x}^{\mathrm{H}}(t),$$

$$\hat{\boldsymbol{R}}_{yy} = \frac{1}{N}\sum_{n=1}^{N} \boldsymbol{y}(t)\boldsymbol{y}^{\mathrm{H}}(t),$$

$$\hat{\boldsymbol{R}}_{xy} = \frac{1}{N}\sum_{n=1}^{N} \boldsymbol{x}(t)\boldsymbol{y}^{\mathrm{H}}(t),$$

and

$$\hat{\boldsymbol{R}}_{yx} = \frac{1}{N}\sum_{n=1}^{N} \boldsymbol{y}(t)\boldsymbol{x}^{\mathrm{H}}(t).$$

Step 2 Eliminate the noises and obtain $\hat{\boldsymbol{C}}_{xx}$ and $\hat{\boldsymbol{C}}_{yy}$.

Step 3 Define $\boldsymbol{R}_1$ and $\boldsymbol{R}_2$ by (14) and (15) respectively, and structure the extended DOA matrix as $\boldsymbol{R}_E = \boldsymbol{R}_2 \boldsymbol{R}_1^{+}$.

Step 4 Implement EVD to $\boldsymbol{R}_E$ and compute the frequency estimates $\hat{f}_k$ and angle estimates $\hat{\theta}_k$ according to (26) and (33).

Remark 2 In this paper, we assume that the source number K is known. If K is unknown, we can utilize the matrix decomposition method, smoothed rank method, Gerschgorin discs method or information theory method to estimate K [32−35].

5. Discussions

5.1 Complexity

For the proposed method, the complexity for each iteration in $\boldsymbol{R}_{xy}$, $\boldsymbol{R}_{yx}$, $\boldsymbol{R}_{xx}$, and $\boldsymbol{R}_{yy}$, costs $O\{4M^2N\}$ in total. The complexity of $\boldsymbol{R}_1^{+}$ and $\boldsymbol{R}_E$ costs $O\{5M^3\}$ and $O\{4M^3\}$, respectively. The complexity of the EVD is $O\{8M^3\}$. Therefore, the complexity of the proposed method is $O\{4M^2N + 17M^3\}$, where N is the number of snapshots.

5.2 Cramer-Rao bound (CRB)

In this subsection, we derive the CRB of the angle and frequency estimation for the received system. We define the data model of the system as

$$z(t) = \begin{bmatrix} \boldsymbol{x}(t) \\ \boldsymbol{y}(t) \end{bmatrix} = \begin{bmatrix} \boldsymbol{A} \\ \boldsymbol{A\Gamma} \end{bmatrix} \boldsymbol{s}(t) + \begin{bmatrix} \boldsymbol{n}(t) \\ \boldsymbol{n}(t-\tau) \end{bmatrix} = \boldsymbol{A}_D \boldsymbol{s}(t) + \boldsymbol{N}(t) \tag{34}$$

where

$$\boldsymbol{A}_D = \begin{bmatrix} \boldsymbol{A} \\ \boldsymbol{A\Gamma} \end{bmatrix},$$

$$\boldsymbol{N}(t) = \begin{bmatrix} \boldsymbol{n}(t) \\ \boldsymbol{n}(t-\tau) \end{bmatrix}.$$

Hence the variance matrix of $z(t)$ is

$$\boldsymbol{R}_{zz} = \mathrm{E}[z(t)z^{\mathrm{H}}(t)]. \tag{35}$$

The signal covariance matrix can be computed as

$$\boldsymbol{\Psi} = \frac{\boldsymbol{s}\boldsymbol{s}^{\mathrm{H}}}{N}. \tag{36}$$

We define the matrix parameter vector $\boldsymbol{\eta} = [\theta_1, \theta_2, \cdots, \theta_K, f_1, f_2, \cdots, f_K]^{\mathrm{T}}$.

Then we can denote the Fisher information matrix (FIM) [36] as

$$\mathrm{FIM} = N\left(\frac{\partial \bar{\boldsymbol{p}}}{\partial \eta}\right)^{\mathrm{H}} (\boldsymbol{P}^{\mathrm{T}} \otimes \boldsymbol{P})^{-1} \frac{\partial \bar{\boldsymbol{p}}}{\partial \eta} \tag{37}$$

where

$$\boldsymbol{P} = \boldsymbol{A}_D \boldsymbol{\Psi} \boldsymbol{A}_D^{\mathrm{H}} + \boldsymbol{I}, \tag{38}$$

$$\bar{\boldsymbol{p}} = \mathrm{vec}(\boldsymbol{P}) = (\boldsymbol{A}_D^* \odot \boldsymbol{A}_D)\boldsymbol{\tau} + \mathrm{vec}(\boldsymbol{I}), \tag{39}$$

$$\frac{\partial \bar{\boldsymbol{p}}}{\partial \eta} = \left[\frac{\partial \bar{\boldsymbol{p}}}{\partial \theta_1}, \frac{\partial \bar{\boldsymbol{p}}}{\partial \theta_2}, \ldots, \frac{\partial \bar{\boldsymbol{p}}}{\partial \theta_K}, \frac{\partial \bar{\boldsymbol{p}}}{\partial f_1}, \frac{\partial \bar{\boldsymbol{p}}}{\partial f_2}, \ldots, \frac{\partial \bar{\boldsymbol{p}}}{\partial f_K}\right]. \tag{40}$$

Hence, by utilizing (36), we can compute

$$\frac{\partial \bar{\boldsymbol{p}}}{\partial \boldsymbol{\eta}} = [\boldsymbol{A}_{s1}\boldsymbol{\Pi}, \boldsymbol{A}_{s2}\boldsymbol{\Pi}] \tag{41}$$

where

$$\boldsymbol{A}_{s1} = (\boldsymbol{D}_1^* \odot \boldsymbol{A}_D + \boldsymbol{A}_D^* \odot \boldsymbol{D}_1), \tag{42}$$

$$\boldsymbol{A}_{s2} = (\boldsymbol{D}_2^* \odot \boldsymbol{A}_D + \boldsymbol{A}_D^* \odot \boldsymbol{D}_2), \tag{43}$$

$$\boldsymbol{D}_1 = \left[\frac{\partial \bar{\boldsymbol{a}}(\theta_1, f_1)}{\partial \theta_1}, \frac{\partial \bar{\boldsymbol{a}}(\theta_2, f_2)}{\partial \theta_2}, \cdots, \frac{\partial \bar{\boldsymbol{a}}(\theta_K, f_K)}{\partial \theta_K}\right], \tag{44}$$

$$\boldsymbol{D}_2 = \left[\frac{\partial \bar{\boldsymbol{a}}(\theta_1, f_1)}{\partial f_1}, \frac{\partial \bar{\boldsymbol{a}}(\theta_2, f_2)}{\partial f_2}, \cdots, \frac{\partial \bar{\boldsymbol{a}}(\theta_K, f_K)}{\partial f_K}\right]. \tag{45}$$

$$\boldsymbol{\Pi} = \mathrm{diag}(\boldsymbol{\tau}). \tag{46}$$

By letting

$$\boldsymbol{F} = (\boldsymbol{P}^{\mathrm{T}} \otimes \boldsymbol{P})^{-\frac{1}{2}} \boldsymbol{A}_d \boldsymbol{R}_0 \tag{47}$$

where $\boldsymbol{A}_d = [\boldsymbol{A}_{d1}, \boldsymbol{A}_{d2}], \boldsymbol{R}_0 = \mathrm{diag}(\boldsymbol{R}_{zz}, \boldsymbol{R}_{zz})$, CRB can be obtained as

$$\mathrm{CRB} = \frac{1}{N}(\boldsymbol{F}^{\mathrm{H}}\boldsymbol{F})^{-1}. \tag{48}$$

5.3 Uniform linear arrays

In this subsection, we discuss the estimation performance of the proposed method for uniform linear arrays. Other things being equal, we define inter-element spacing as d. Hence, $\boldsymbol{A}$ can be reformulated into

$$\boldsymbol{A}' = \begin{bmatrix} 1 & 1 & \cdots & 1 \\ \mathrm{e}^{-\mathrm{j}2\pi f_1 d \frac{\sin\theta_1}{\mathrm{c}}} & \mathrm{e}^{-\mathrm{j}2\pi f_2 d \frac{\sin\theta_2}{\mathrm{c}}} & \cdots & \mathrm{e}^{-\mathrm{j}2\pi f_K d \frac{\sin\theta_K}{\mathrm{c}}} \\ \vdots & \vdots & \ddots & \vdots \\ \mathrm{e}^{-\mathrm{j}2\pi f_1 (M-1) d \frac{\sin\theta_1}{\mathrm{c}}} & \mathrm{e}^{-\mathrm{j}2\pi f_2 (M-1) d \frac{\sin\theta_2}{\mathrm{c}}} & \cdots & \mathrm{e}^{-\mathrm{j}2\pi f_K (M-1) d \frac{\sin\theta_K}{\mathrm{c}}} \end{bmatrix}. \tag{49}$$

Replacing the matrix $\boldsymbol{A}$ with $\boldsymbol{A}'$ in (3)−(25), we can obtain the frequency estimation (26).

For a uniform linear array, (27), (28), and (30) can be rewritten as

$$\boldsymbol{a}(\theta_k) = \left[1, \mathrm{e}^{-\mathrm{j}2\pi d f_k \frac{\sin\theta_k}{\mathrm{c}}}, \cdots, \mathrm{e}^{-\mathrm{j}2\pi(M-1) d f_k \frac{\sin\theta_k}{\mathrm{c}}}\right]^{\mathrm{T}}, \tag{50}$$

$$\boldsymbol{u}_k = -\mathrm{angle}(\boldsymbol{a}(\theta_k)) = \left[0, 2\pi d f_k \frac{\sin\,\theta_k}{\mathrm{c}}, \cdots, 2\pi(M-1) d f_k \frac{\sin\,\theta_k}{\mathrm{c}}\right]^{\mathrm{T}}, \tag{51}$$

$$\begin{cases} \boldsymbol{P}_k = \begin{bmatrix} 1 & 0 \\ 1 & 2\pi d \dfrac{\hat{f}_k}{\mathrm{c}} \\ \vdots & \vdots \\ 1 & 2\pi(M-1) d \dfrac{\hat{f}_k}{\mathrm{c}} \end{bmatrix} \\ \boldsymbol{e}_k = \begin{bmatrix} e_0 \\ e_1 \end{bmatrix}, \end{cases} \tag{52}$$

where $\hat{f}_k$ is the estimation of the frequency and $e_1 = \sin\,\theta_k$.

5.4 Advantages

The proposed method has the following advantages:

(i) The parameter estimation performance of the proposed method is superior to the conventional DOAM method.

(ii) The proposed method adequately utilizes the autocorrelation and cross-correlation information to construct the extended DOA matrix, while the conventional DOAM method partly exploits the information.

(iii) The proposed method suits both non-uniform and uniform arrays.

6. Simulation results

We consider the signal receiving system with single delay and suppose $K=3$ sources impinge on the linear array. These sources located at angles $\theta_1=10°$, $\theta_2=20°$, and $\theta_3=30°$, with $f_1=6$ MHz, $f_2=8$ MHz, and $f_3=10$ MHz. K, M, and N are the number of sources, array elements, and snapshots, respectively. In the following simulations, $c=3\times10^8$ m/s is the signal propagation velocity. The delay of system is $\tau=40$ ns. We assess the angle and frequency estimation performance of the proposed method by the root mean square error (RMSE) as

$$\mathrm{RMSE}=\frac{1}{K}\sum_{k=1}^{K}\sqrt{\frac{1}{1\,000}\sum_{i=1}^{1\,000}(\hat{\theta}_{k,i}-\theta_k)^2}, \tag{53}$$

$$\mathrm{RMSE}=\frac{1}{K}\sum_{k=1}^{K}\sqrt{\frac{1}{1\,000}\sum_{i=1}^{1\,000}(\hat{f}_{k,i}-f_k)^2}, \tag{54}$$

where θ_k and f_k are the accurate DOA and frequency of the kth source. $\hat{\theta}_{k,i}$ and $\hat{f}_{k,i}$ are the estimates of θ_k and f_k in the ith Monte Carlo simulation. In this paper, we set the total times of the Monte Carlo simulation trials as $I=1\,000$.

Fig. 3 shows the estimation consequences of our proposed method for a uniform linear array while the distance between any two adjacent array elements is $d=12$ m. It depicts that our proposed method can accurately achieve joint estimation of DOA and frequency for uniform linear array.

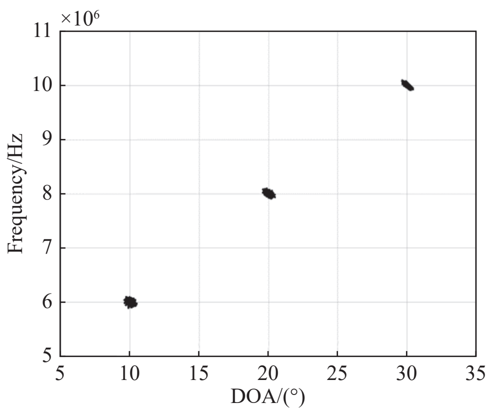

Fig. 3 Angle and frequency scatter with uniform linear array

Fig. 4 and Fig. 5 present the RMSE comparison of our proposed method and some other method for uniform linear array, where $M=12$, $K=3$, and $N=500$. We find the proposed algorithm can also work well in the case of uniform linear arrays. Furthermore, the proposed method is more accurate than the conventional DOAM method [20] and the PM algorithm [18]. From Fig. 4 and Fig. 5, it is shown that IM-ESPRIT performs slightly better than our proposed method.

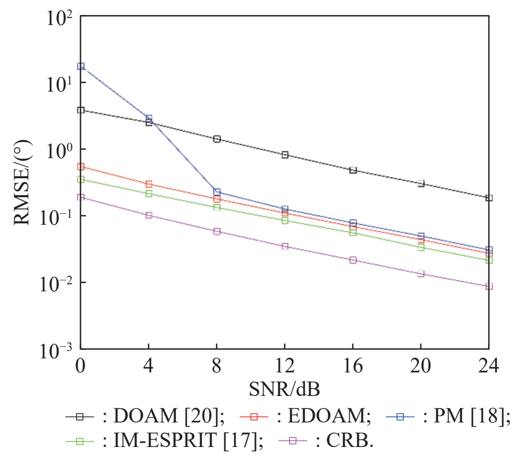

Fig. 4 RMSE of angle estimation with different SNRs for uniform linear array

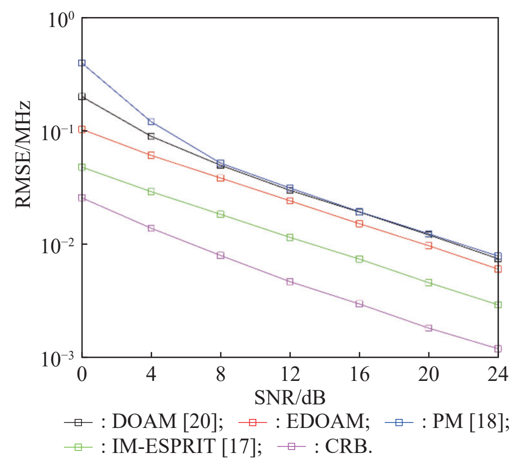

Fig. 5 RMSE of frequency estimation with different SNRs for uniform linear array

Fig. 6 and Fig. 7 show the DOA and frequency estimation precision of the proposed method under different snapshots N for uniform linear array, where SNR = 10 dB, $M=12$, and $K=3$. Fig. 6 and Fig. 7 indicate that the estimation accuracy of both angle and frequency improves as the number of snapshots N increasing. Furthermore, these reconfirm that the proposed method has higher angle and frequency estimation precision than the conventional DOAM method [20] and the PM algorithm [18].

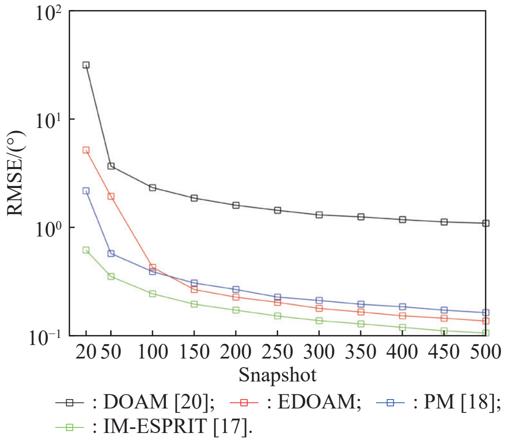

Fig. 6 RMSE of angle estimation with different snapshots for uniform linear array

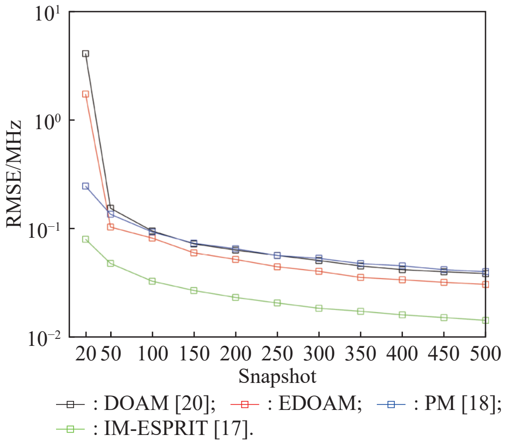

Fig. 7 RMSE of frequency estimation with different snapshots for uniform linear array

Fig. 8 presents the estimation results of our proposed method for a non-uniform linear array, where SNR = 10 dB, $N = 500$, $M = 12$, $K = 3$. Fig. 8 is a non-uniform array design example where the elements positions are $d = \{0\ 9.6\ 16.8\ 30\ 45.6\ 54\ 60\ 73.2\ 84\ 99.6\ 117\ 60\ 73.2\ 84\ 99.6\ 117\ 140.4\}$. Fig. 8 explicitly shows that our proposed method can accurately achieve joint estimation of DOA and frequency. Fig. 9 and Fig. 10 depict the angle and frequency estimation performance comparison of the proposed method and the traditional DOAM method [20] for a non-uniform linear array, where $N = 500$, $M = 12$, and $K = 3$. Fig. 4 and Fig. 5 show clearly that our proposed method has higher angle and frequency estimation precision compared to the conventional method since the conventional DOAM method [20] partly ignores the information of the auto-correlation and the cross-correlation matrices while the proposed method gets the utmost out of the information. IM-ESPRIT fails to work in a non-uniform linear array, and then we have not shown IM-ESPRIT in Fig. 8 and Fig. 12.

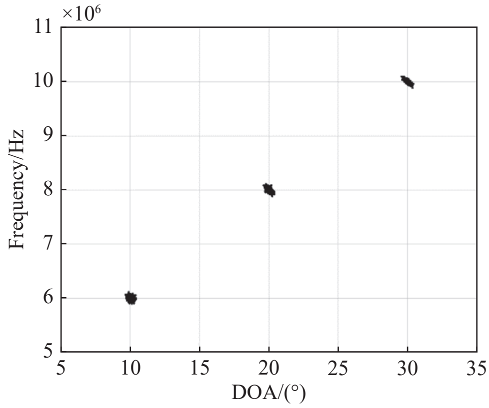

Fig. 8 Angle and frequency scatter with non-uniform linear array

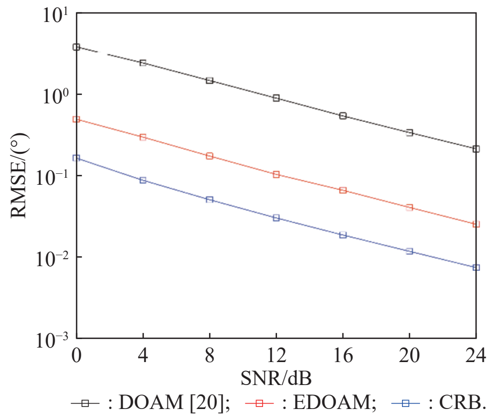

Fig. 9 RMSE of angle estimation with different SNRs for non-uniform linear array

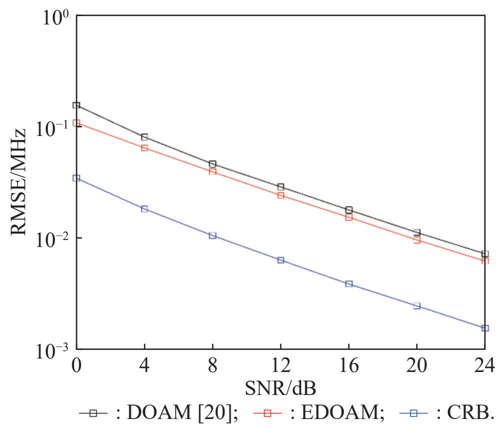

Fig. 10 RMSE of frequency estimation with different SNRs for non-uniform linear array

Fig. 11 and Fig. 12 illustrate the DOA and frequency estimation accuracy of the proposed method under different snapshots N for a non-uniform linear array, where signal-to-noise ratio SNR = 10 dB, $M = 12$, and $K = 3$. It can be observed that the estimation performance of both angle and frequency improves with the increase of snapshots N. Furthermore, these reconfirm that the proposed method is more precise than the conventional DOAM method [20] with all the snapshots.

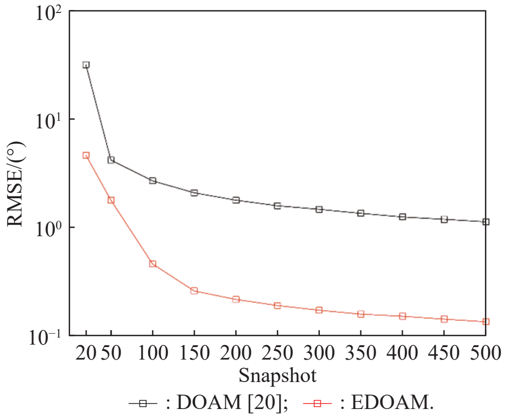

Fig. 11 RMSE of angle estimation with different snapshots for non-uniform linear arrays

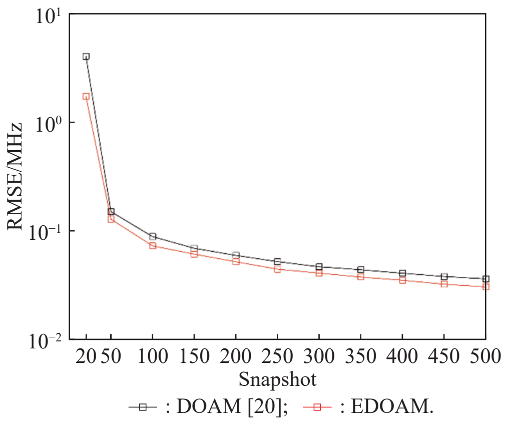

Fig. 12 RMSE of frequency estimation with different snapshots for non-uniform linear arrays

7. Conclusions

In this paper, we propose the EDOAM method to jointly estimating the angle and frequency. The proposed method constructs EDOAM which makes the best of all cross-correlation and autocorrelation information, while the conventional DOA-Matrix method ignores part of the information. We can obtain the auto-paired frequency and angle estimates by the eigenvalues and the corresponding eigenvectors of the EDOAM. The emulation consequences demonstrate that the proposed method estimation precision outperforms the conventional DOA-Matrix method.

References

[1] JACKSON L, CHIEN H. Frequency and bearing estimation by two-dimensional linear prediction. Proc. of the IEEE International Conference on Acoustics, Speech, and Signal Processing, 1979: 665–668.

[2] ZOLTOWSKI M D, MATHEWS C P. Real-time frequency and 2-D angle estimation with sub-Nyquist spatio-temporal sampling. IEEE Trans. on Signal Processing, 1994, 42(10): 2781–2794.

[3] HAARDT M, NOSSEK J A. 3-D unitary ESPRIT for joint 2-D angle and carrier estimation. Proc. of the IEEE International Conference on Acoustics, Speech, and Signal Processing, 1997: 255–258.

[4] STROBACH P. Total least squares phased averaging and 3-D ESPRIT for joint azimuth-elevation-carrier estimation. IEEE Trans. on Signal Processing, 2001, 49(1): 54–62.

[5] YU H X, ZHANG X F, CHEN X Q, et al. Computationally efficient DOA tracking algorithm in monostatic MIMO radar with automatic association. International Journal of Antennas and Propagation, 2014, 2014: 501478.

[6] SCHMIDT R. Multiple emitter location and signal parameter estimation. IEEE Trans. on Antennas and Propagation, 1986, 34(3): 276–280.

[7] ROY R, KAILATH T. ESPRIT-estimation of signal parameters via rotational invariance techniques. IEEE Trans. on Acoustics, Speech, and Signal Processing, 1989, 37(7): 984–995.

[8] STOICA P, HANDEL P, SODERSTROM T. Study of Capon method for array signal processing. Circuits, Systems and Signal Processing, 1995, 14(6): 749–770.

[9] TAYEM N, KWON H M. L-shape 2-dimensional arrival angle estimation with propagator method. IEEE Trans. on Antennas and Propagation, 2005, 53(5): 1622–1630.

[10] CLARK M P, SCHARF L L. Two-dimensional modal analysis based on maximum likelihood. IEEE Trans. on Signal Processing, 1994, 42(6): 1443–1452.

[11] YIN Q Y, NEWCOMB R W, ZOU L H. Estimating 2-D angles of arrival via two parallel linear arrays. Proc. of the International Conference on Acoustics, Speech, and Signal Processing, 1989: 2803–2806.

[12] YIN Q Y, NEWCOMB R W, MUNJAL S, et al. Relation between the DOA matrix method and the ESPRIT method. Proc. of the IEEE International Symposium on Circuits and Systems, 1990: 1561–1564.

[13] LIN J D, FANG W H, WANG Y Y, et al. FSF MUSIC for joint DOA and frequency estimation and its performance analysis. IEEE Trans. on Signal Processing, 2006, 54(12): 4529–4542.

[14] OGAWA Y, HAMAGUCHI N, OHSHIMA K, et al. High-resolution analysis of indoor multipath propagation structure. IEICE Trans. on Communications, 1995, E78B(11): 1450–1457.

[15] WANG Y Y, CHEN J T, FANG W H. TST-MUSIC for joint DOA-delay estimation. IEEE Trans. on Signal Processing, 2001, 49(4): 721–729.

[16] WANG X D. Joint angle and frequency estimation using multiple-delay output based on ESPRIT. EURASIP Journal on Advances in Signal Processing, 2010, 2010(1): 358659.

[17] WANG X D, ZHANG X F, LI J F, et al. Improved ESPRIT method for joint direction-of-arrival and frequency estimation using multiple-delay output. International Journal of Antennas and Propagation, 2012, 2012: 309269.

[18] SUN Z W, ZHANG X F, WU H L, et al. Propagator method-based joint angle and frequency estimation using multiple delay output. ICIC Express Letters, 2011, 2(4): 827–832.

[19] WAX M, LESHEM A. Joint estimation of time delays and

directions of arrival of multiple reflections of a known signal. IEEE Trans. on Signal Processing, 1997, 45(10): 2477–2484.
[20] WANG S, ZHOU X L. Direction-of-arrival and frequency estimation in array signal processing. Journal of Shanghai Jiaotong University, 1999, 33(1): 40–42. (in Chinese)
[21] ZOLTOWSKI M D, HAARDT M, MATHEWS C P. Closed-form 2-D angle estimation with rectangular arrays in element space or beamspace via unitary ESPRIT. IEEE Trans. on Signal Processing, 1996, 44(2): 316–328.
[22] DAI X R, ZHANG X F, WANG Y F. Extended DOA-matrix method for DOA estimation via two parallel linear arrays. IEEE Communications Letters, 2019, 23(11): 1981–1984.
[23] YAO B B, WANG W J, YIN Q Y. DOD and DOA estimation in bistatic non-uniform multiple-input multiple-output radar systems. IEEE Communications Letters, 2012, 16(11): 1796–1799.
[24] PAL P, VAIDYANATHAN P P. Nested arrays: a novel approach to array processing with enhanced degrees of freedom. IEEE Trans. on Signal Processing, 2010, 58(8): 4167–4181.
[25] DU R Y, WANG J K, LIU F L. Space-time matrix method for joint frequency and 2-D DOA estimation. Proc. of the International Conference on Information Science and Engineering, 2009: 671–674.
[26] XU L Y, ZHANG X F, XU Z Z. Joint 2D angle and frequency estimation method based on parallel factor quadrilinear decomposition. Journal of Electronics & Information Technology, 2011, 33(8): 1889–1894. (in Chinese)
[27] LI S, SUN Z Z, ZHANG X F, et al. Joint DOA and frequency estimation for linear array with compressed sensing PARAFAC framework. Journal of Circuits, Systems and Computers, 2017, 26(9): 1750136.
[28] SHAFIN R, LIU L J, LI Y, et al. Angle and delay estimation for 3-D massive MIMO/FD-MIMO systems based on parametric channel modeling. IEEE Trans. on Wireless Communications, 2017, 16(8): 5370–5383.
[29] LIN J C, MA X C, YAN S F, et al. Time-frequency multi-invariance ESPRIT for DOA estimation. IEEE Antennas and Wireless Propagation Letters, 2016, 15: 770–773.
[30] WU R H, XU L, ZHANG Z H, et al. Joint 2-D DOA and Doppler estimation for L-shaped array via dual PARAFAC with triple matching implementation. IEEE Access, 2019, 7: 51749–51758.
[31] XU L, WU R H, ZHANG X F, et al. Joint two-dimensional DOA and frequency estimation for L-shaped array via compressed sensing PARAFAC method. IEEE Access, 2018, 6: 37204–37213.
[32] DI A Z. Multiple source location—a matrix decomposition approach. IEEE Trans. on Acoustics, Speech, and Signal Processing, 1985, 33(5): 1086–1091.
[33] HUANG L, LONG T, MAO E, et al. MMSE-based MDL method for robust estimation of number of sources without eigendecomposition. IEEE Trans. on Signal Processing, 2009, 57(10): 4135–4142.
[34] HSIEN-TSAI W, JAR-FERR Y, FWU-KUEN C. Source number estimator using Gerschgorin disks. Proc. of the IEEE International Conference on Acoustics, Speech and Signal Processing, 1994: 261–264.
[35] ZHENG C D, FENG D Z, ZHOU Y. Detection of number of sources via exploitation of non-circular property. Journal of Xidian University, 2006, 33(3): 466–470. (in Chinese)
[36] STOICA P, NEHORAI A. MUSIC, maximum likelihood, and Cramer-Rao bound. IEEE Trans. on Acoustics, Speech, and Signal Processing, 1989, 37(5): 720–741.

Biographies

CHEN Luo was born in 1986. He received his B.S. degree from Nanchang University, Nanchang, China, in 2007. He received his M.S. degree in internet computing from University of Abertay Dundee, Dundee, UK, in 2010. He is currently pursuing his Ph.D. degree at the College of Electronics and Information Engineering, Nanjing University of Aeronautics and Astronautics, Nanjing, China. He is also working at the 28th Research Institute of China Electronics Technology Group Corporation, Nanjing , China. His research interests include array signal processing and communication signal processing.
E-mail: njxnd88@126.com

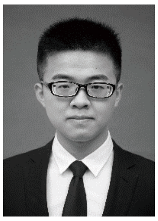

DAI Xiangrui was born in 1997. He received his B.E. degree from Anhui University, Hefei, China, in 2018. He is currently pursuing his M.S. degree in electronic and communications engineering with the College of Electronic and Information Engineering at Nanjing University of Aeronautics and Astronautics, Nanjing, China. His current research interests include array signal processing and communication signal processing.
E-mail: xr.dai@foxmail.com

ZHANG Xiaofei was born in 1977. He received his M.S. degree from Wuhan University, Wuhan, China, in 2001. He received his Ph.D. degree in communication and information systems from Nanjing University of Aeronautics and Astronautics in 2005. He is a full professor of the College of Electronics and Information Engineering, Nanjing University of Aeronautics and Astronautics, Nanjing, China. His research focuses on array signal processing and communication signal processing.
E-mail: zhangxiaofei@nuaa.edu.cn